Journal of Multidisciplinary Engineering Science and Technology (JMEST)
ISSN: 2458-9403
Vol. 3 Issue 7, July - 2016

Preparing A Mesoporous Silicon As A Photodetector By Electrochemical Etching Process

Duha M.A. Latif
Physics Department, Education Faculty , Baghdad University, Baghdad,Iraq

***Abstract*—In this work, p-type porous silicon was prepared as a photodetector from p-type crystalline silicon with (100) orientation by an electrochemical etching process with 25.5 mA/cm^2 etching current density for 10 min etching time. The structural, morphological, chemical and electrical properties was studied. From the electrical measurements the ideality factor (n) was found to be 3.7, the rectification ratio (R_f) equal to 462.09 and the built in potential was 1.2 V. PL measurements shows that the energy gap of etched silicon increased from 1.12 to 1.65 eV. From current voltage (I-V) characteristics, the illuminated current increase with increasing the incident power under reverse biasing and this refer to good responsivity to the incident photons.**

Keywords—mesoporous, ideality factor, built-in potential, responsivity and detectivity.

1.Introduction: Nowadays, mostly photons instead of electrons are used as information carriers due to their lower interaction with matter resulting in higher speed and lower power consumption. Silicon with its indirect electronic band gap has only poor light emitting capabilities [1] [2] . Porous materials are characterized by a large surface-to-volume ratio and controlling the size of the building blocks (e.g. the walls as well as the voids) is of interest, too. This can improve the performance of the structures and open up new fields of application, e.g. as template materials or as photonic crystals[3]. For nearly a decade, world-wide efforts have been directed toward the study of silicon nanocrystals in the sub-microns to nanometer size regime[4][5][6].This interest resulted from the first observation in 1990, of visible, room temperature lumin-escence emanating from porous silicon[7] . Porous silicon is an intriguing materials because it is based on a silicon structure that is known to be a very inefficient light emitter, which is characterized of indirect band gap semiconductor[8]. The porous silicon matrix is characterized by the dimensions of the pores, ranging from the micro porous ($d_{pore} < 2$ nm), mesoporous ($2 < d_{por\ e} < 50$ nm) and macro porous ($d_{por\ e} > 50$nm)[9]. In 1956, Uhlir first demonstrated that porous silicon can be electrochemically formed in an hydrochloric acid (HF) based electrolyte[10]. The main requirements in the formation of porous silicon ar: (1)the silicon wafer must be anemically biased: (2) current densities below a critical value must be used, the first condition result because holes are consumed during the etching of silicon, when the second condition is violated, electropolising occurs, whereby holes pile up on the silicon-HF interface and layers of silicon atoms are removed[8]. The formation of micro porous silicon is a result of quantum confinement effects [7][11] . It is independent of doping and crystal orientation and a layer of micro porous silicon often covers the walls of meso- or macrospores. For the mesoporous and macroporous structures the formation of a space charge region (SCR) in an electrochemical setup is necessary. Mesopores are formed mainly by tunneling processes within the SCR[12], while macrospores are formed as a result of thermionic emission (for p-type doping)[13] or the collection of minority charge carriers (for n-type doping)[14][15]. Porous silicon (PS) consists of a network of nanoscale sized silicon wires and voids which formed when crystalline silicon wafers are etched electrochemically in hydrofluoric acid based electrolyte solution under constant anodization conditions like etching time , current density , HF concentration and Si orientation[16]. The optical properties of porous silicon (direct gap, low reflectivity, variable refractive index, photoluminescence, randomized morph -ological structure and possibility of band gap engineering) make this material to be a good candidate for photovoltaic applications[17][18].

2-Experimental part:

Mirror -like single crystalline Si substrates with electrical resistivity (10Ω.cm) and (100) orientation have been used in this work. The porous layer was prepared by electrochemical etching process carried out by using home-made Teflon cell with an electrolyte containing 48% HF and 99.9% ethanol, 1:1 by volume as show in figure(1). The substrates were cut into square with areas of (1.5cm×1.5cm). high purity Al film was deposited by using thermal evaporation technique with thickness (0.1μm). The silicon sample was etched at 25.5mA/cm^2 current density for 10min etching time at room temperature. After anodization, the silicon samples were washed out with deionized water for 5 minutes and dried under N_2 ambient.

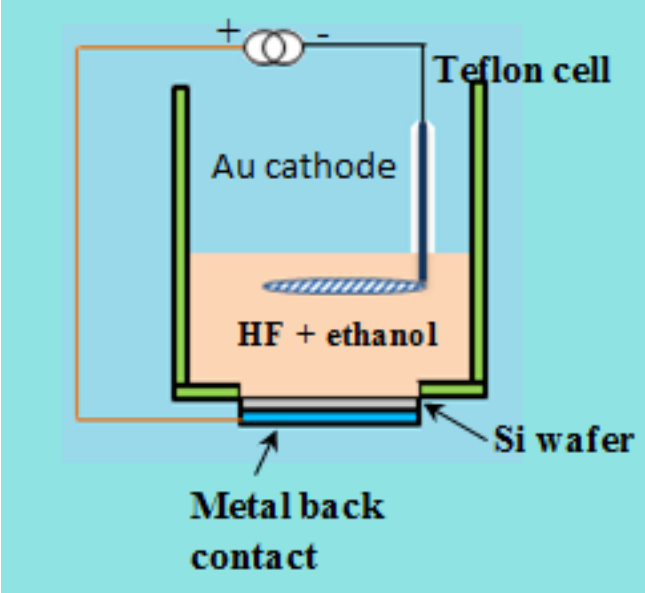

Fig(1): Cross-sectional view of electrochemical etching cell

Fig.2 shows the cross-sectional view of porous silicon photodeector. The structural, morphological and optical properties of porous silicon were investigated by means of (CuKα) XRD-6000, Shimadzu x-ray diffractometer, Shimadzu SL 174 PL. spectrophotometer, Fourier transformation infrared spectro-scopy, JEOL (JSM-5600) scanning electron microscopy and Angstrom AA 3000 atomic force microscopy. The spectral responsivity of the photodetectors was measured in the range of 400-950 nm by using a monochromator, and a Sanwa silicon power meter was used for monochromator calibration. All the above characteristics are investigated at room temperature.

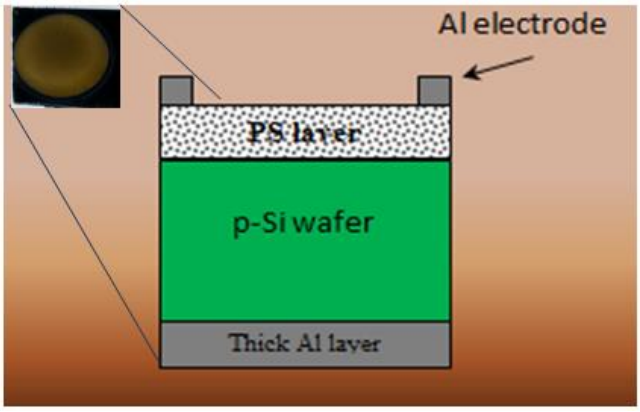

Fig.(2): Cross-sectional view of porous silicon photodetector, the inset represent photographic image of PS photodetector

3. Results and Discussions

Figure (3) shows the microstructure of PS samples prepared at 25.5mA/cm² current density for 10 min etching time by using optical microscopy. This micrograph exhibits that the pore distributed randomly along the surface of the sample and the morphology of

the sample can recognized easily through the films homogeneity and color, also the etched surfaces are rough. The red color was attributed to the oxidization of the PS sample spontaneously when exposed to the ambient air.

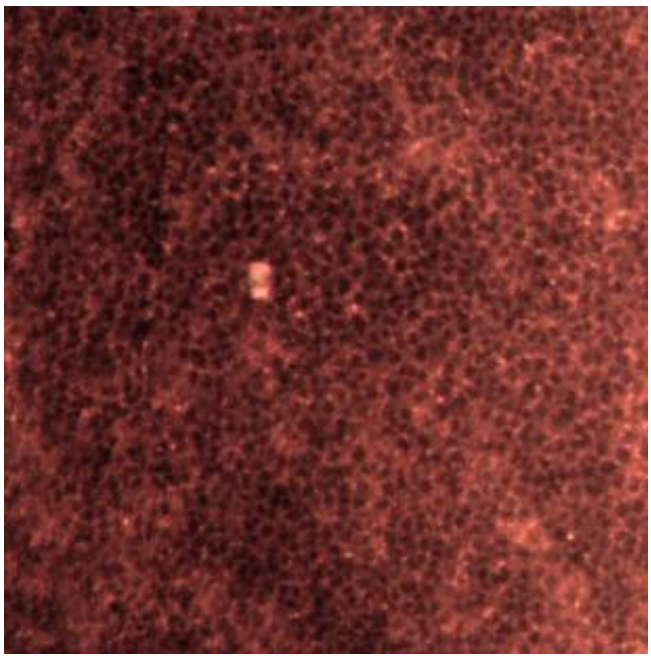

Fig.(3): Optical micrographs of p-PS photodetector, (M=1000).

Figure (4) shows X-ray diffraction of (a) crystalline silicon and (b) PS samples. A peak of PS at 25.5mA/cm^2 current density shows a splitting peak at 2θ = 33.6° oriented only along the (211) direction is observed confirming the monocrystalline structure of the PS layer (according to ICDD N 1997 and 2011

JCPDS).The intensity of the porous silicon peak decreases when crystal size is reduced toward nanometric scale, then a broadening of the peak is observed, as compared with c-Si peak, and the width of the peak is directly correlated to the size of the nanocrystalline domains. This result is ascribed and listed in Table (1).

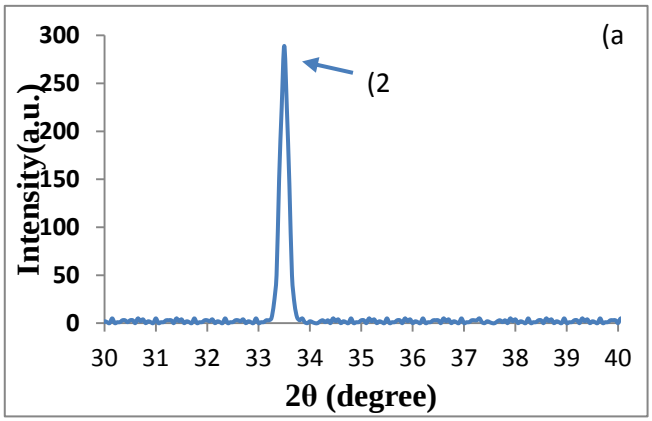

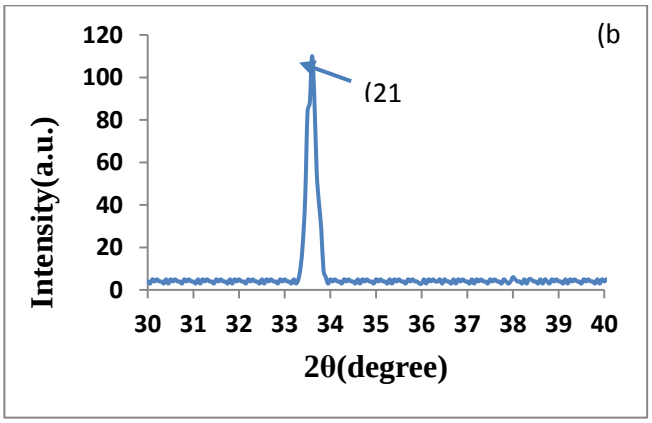

Fig. (4): XRD spectra of (a)c-Si and (b) PS sample

Table 1: Calculated crystallite size, average grain size, dislocation density and strain for PSi prepared at 25.5mA/cm^2 etching current density .

Anodization current density (mA/cm^2)	*2Θ (deg)*	*FWHM (deg)*	*D_{XRD} (nm)*	*D_{AFM} (nm)*	*Dislocation density (lines.m^{-2}) *10^{14}*	*Strain (lines^2 m^{-4}) x10^{-3}*
25.5	**33. 6**	**0.372**	**23.29**	**25.52**	**18.4**	**15.5**

Figure (5) shows the top view SEM image of the PS, the dark spots on the image are attributed to the formed pores, whereas the white area

15 min

onds to the remaining Si (pore wall). The pores are spherical and irregular in shape, and are randomly distributed on the PS surface, this result similar to [19].

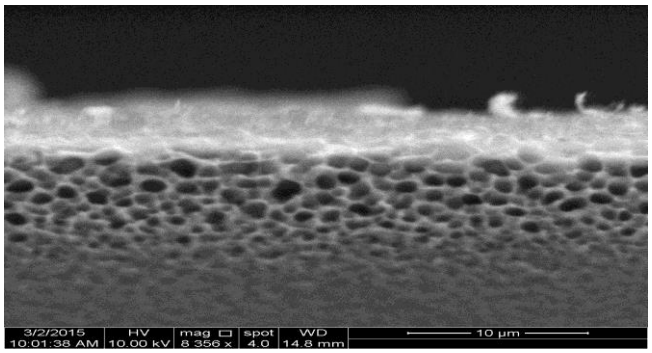

Fig. (5): SEM images (top view) of samples prepared at 10min with 25.5mA/cm^2 etching current density.

AFM images give the formation of uniform porous structures on the Si wafer. The morphological properties of the PS sample prepared with current density 25.5mA/cm^2 at 10min etching time is shows in figure (6), which show

3D and 2D images of the anodized PS. From this figure the average diameter found to be 25.52nm (i.e. the porous type is mesoporous), the average roughness is 0.36nm and the RMS is 0.442nm, while the Porosity equal to 68%.

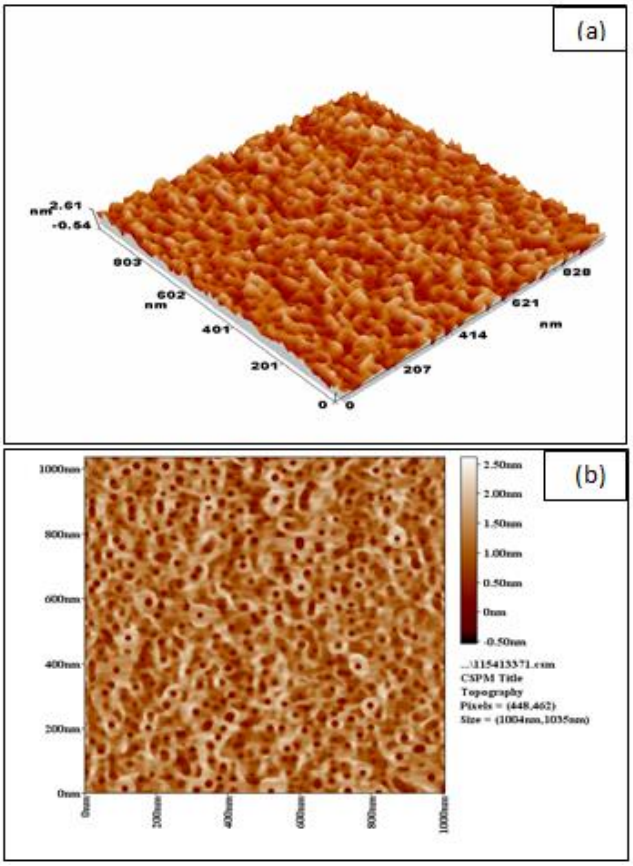

Fig.(6): (a)3D and(b) 2D AFM images of p-PS surface

Surface chemical composition of PSi is best probed with Fourier Transform Infrared (FTIR) spectroscopy. Figure (7) shows the FTIR spectra measured from sample of at different current densities. A strong broad band is observed at about 1071 cm^{-1} and 1080.17 cm^{-1} due to Si-O-Si asymmetry stretching vibrations mode in PSi , which are dependent on the oxidation degree of porous silicon. The transm-ittance peak at 624.94 cm^{-1}, 638.46 cm^{-1} , 873 cm^{-1} , 2088.98 cm^{-1}, 2114.05 cm^{-1} and 2260.65 cm^{-1} Si-H bending in (Si_3SiH), 908.47 cm^{-1} Si-H_2 scissor mode. The transmittance peak at 1705.07 cm^{-1} related to C-O.

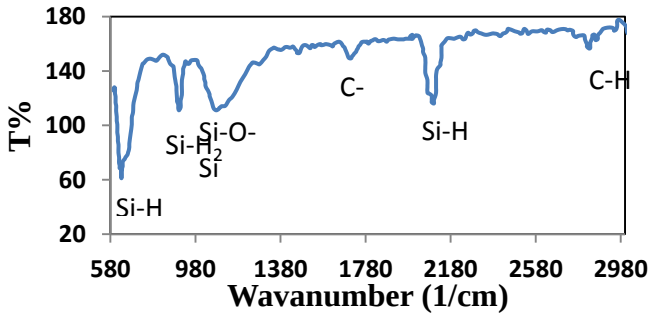

Fig. (7): FTIR spectra of the sample prepared at 10 min for 25.5mA/cm2 etching current density.

PL spectrum of the PS/p-Si photo-detector formed at the etching current density 25.5mA/cm^2 for 10 min etching time indicating emission peak

748 nm as shows in figure (8), the PL peak are related to the S-band emission, an emission for the fixed excitation wavelength at 380 nm.

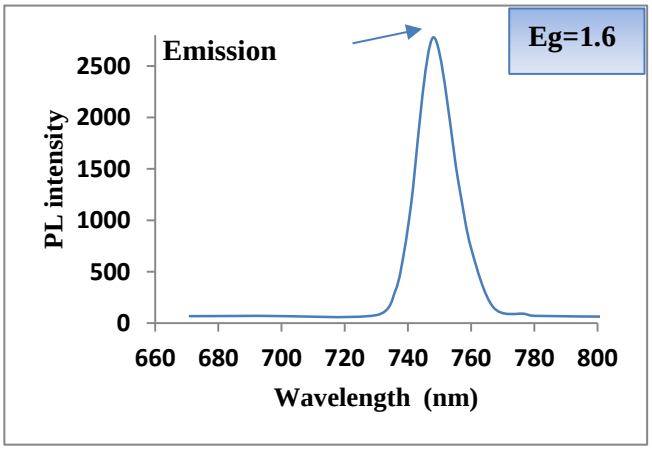

Fig. 8: PL spectra for p-PSi prepared at 10 min etching time and 25.5mA/cm2 current density.

The high porosity and thereby large porous structures leads to brighter PL at shorter wavelengths , and this may be attributed to the luminescence from the confined silicon structures (large energy gap with small crystalline size), size dependency of the PL energy, which explains the efficient luminescence[20].

Figure(9) represents the (I-V) characteristics of the PS photodetector, were obtained by applying bias (sweeping from -10V to +10V), this figure can be explained the non-linear behavior(at low voltage),that is mean under the forward bias condition it shows the exponential increase in current. Under reverse bias reverse current is slightly increased with the applied voltage and this leads to generate electron-hole pairs at low bias. The forward current of all

photodetector is very small at voltage less than 2 V. This current is known as recombination current which occurs at low voltages only. It is generated when each electron excited from valence band to get the balance back. The second region at high voltage represents the diffusion or bending region which depending on serried resistance. In this region, the bias voltage can deliver electrons with enough energy to penetrate the barrier between the two sides of the junction. This result agree with [21]

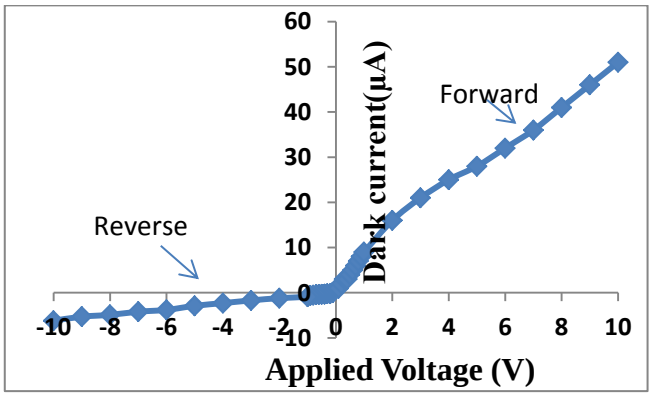

Fig.(9):The Current -Voltage characteristics of PS photodetector .

The ideality factor of the PS photodetector prepared with 25.5 mA / cm^2 etching current density along 10min etching time is 3.7, the ideality factor can be calculated from thermionic emission equation which given by : [22]

$$I(V) = I_s[\exp\left(\frac{qV}{nKT} - 1\right). \quad (1)$$

Where V is the voltage across the device, n is the ideality factor(which is equal to 1. For the ordinary Schottky devices, it is a parameter which can show the ideality of fabricated devices), K is the Boltzmann constant and Is is the saturation current, which obtained from the semi-log forwarded bias as shown in figure (10).

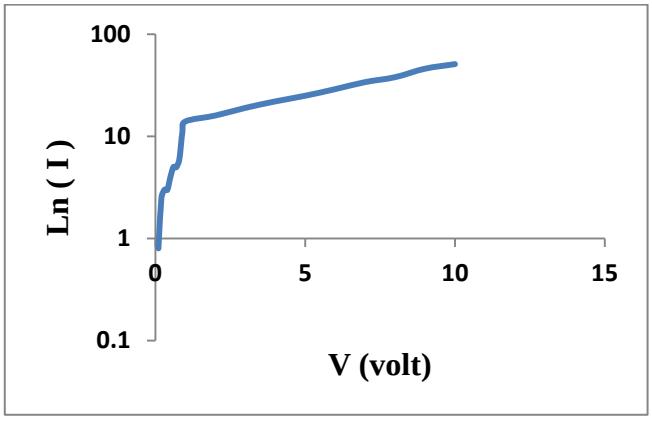

Fig. (10): Ln (I) versus V graphic

Figure (11) explains the photocurrent characteristics of a sandwich structure under illumination with different power densities (313.4, 1323.4, 2723.4 and 5043.3) μW. The photocurrent increase with increasing applied power and this refer to good responsivity to the incident photons, the optimum value of photocurrent is 2865μA at -10V biasing under 5043.3μW. the prepared photodetector has Rectif-ication ratio equal to 462.09.

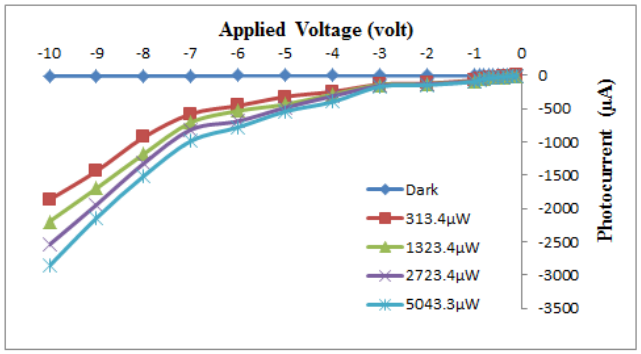

Fig (11): Photocurrent as a function of the applied reverse voltage for Al/PS/p-Si/Al heterojunction .

Figure (12) shows the C-V characteristics of the prepared sandwich structure, the high porosity cause to decreases the capacitance of the PS layer. This behavior was attributed to the increase of the depletion region width which leading to the enhancement of built-in potential 1.12eV. The relation between inverse capacitance squared against the reverse bias is shown in Figure (12) represents that the junction was an abrupt type.

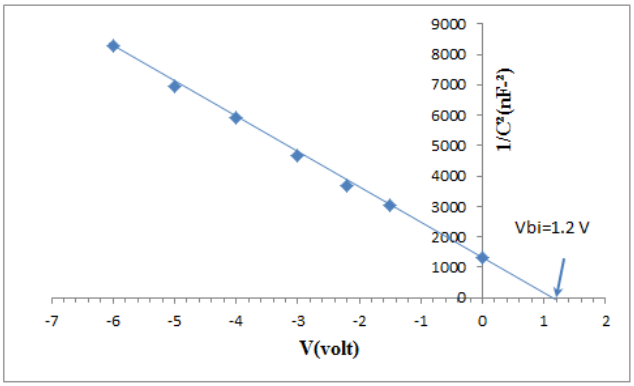

Fig (12): The inverse capacitance squared verses voltage

Figure(13) exhibits the spectral responsivity (R_λ) as a function of wavelength (400–950) nm plot for photodetector with 5V bias. The high responsivity of photodetector 0.65AW^{-1} located at 800nm is arise from a fact that the surface of the porous is ideal in catching photons and the surface is well passivity with very low concentration of surface recombination as well as the reflectivity of porous silicon for visible and near infrared regions is very low and that agree with R. Ismail[23].

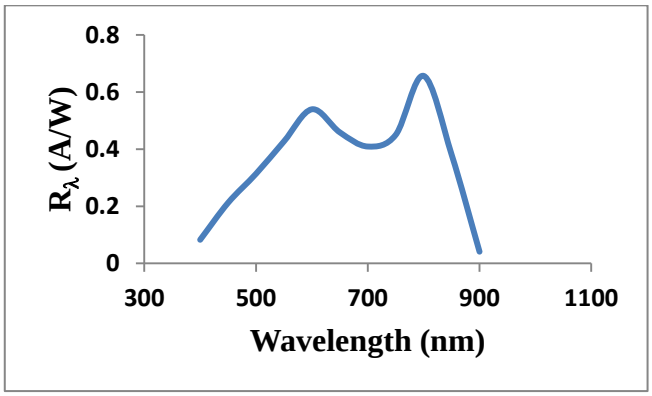

Fig .(13): Spectral responsivity as a function of various incident wavelengths for structure PS/p-Si photodetector.

Figure(14) illustrations the specific detectivity (D*) of the Al/PS/p-Si/Al Photodetector was measured at room temperature as a function of incident light wavelength. and, the maximum value is about $72.7 \times 10^{12} cm.Hz^{1/2}W^{-1}$ at 800nm. The high detectivity of the device indicates increasing the responsivity and a good photodetector is fabricated .

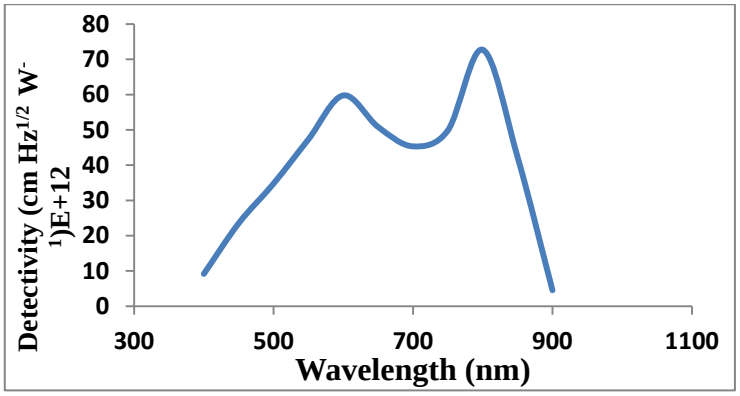

Fig.(14): Measured specific detectivity of the Al/ PS/p-Si/Al photodetector versus wavelength of incident light.

4. Conclusion

From this work it can be concluded that the prepared photodetector was mesoporous and had high porosity 68%, the ideality factor 3.7 , i.e. the prepared photodetector approach from an ideal diode. From the electrical properties of Al/psi/c-Si/Al sandwich, the junction type was abrupt junction and the photocurrent increase with increasing the incident power so that the photodetector has good photoresponse in both visible and near IR regions, with a sensitivity of 0.65 AW^{-1} at 800 nm. The high performance of photodetectors suggests simple, stable and reliable etching technique was used.

References

[1] S.Prucnal, J. Sun, W.Skorupa, and M. Helm, switchable two-colar electroluminescence based on a Si metal-oxide-semiconductor structure doped withEu , Appl. phys. 90 (2007).

[2] R. J. Walters, G.I.Bourianoff, and H.A. Atwater, field –effect

Electroluminescence in silicon nano-crystals, Nat.Mater.4 (2005) 143-146.

[3] M.E. Davis, Orderedporous materaials for emerging application, Nature.417 (2002) 813-821.

[4] P.M. Fauchet, photoluminescence and Electrolumines cencefrom porous silicon, J.Lumin .70 (1996) 38-41.

[5] A.Cullis, L.Canham, and P.Calcott, The structural and luminescence properties of porous silicon , J.Appl. Phys.82 (1997) 67-72.

[6] R.Collins, P.Fauchet and M. Tischler ,prous silicon from luminescence to LED, Phys.Today .50 (1997) 22-31.

[7] L. Canham , Sillicon quantum wir array fabrication by electrochemical and chemical dissolution of water, Appl.Phys. Lett. 57 (1990) 1046-1048.

[8] S.Chan, Porous Sillicon Multilayer Strutures from interference filter to light emitting devices to biosensors , Rochester (2000).

[9] M. Thust, M.J. Schoning , S.Frohnhoff, R. Arens-Fischer, P. Kordos and H. Luth, porous silicon as a substrate material for potentiometric biosensors, Meas .Sci. Technol 7 (1996) 26-29.

[10] A.Uhlir, Electrolytic shaping of Germanium and Sillicon, Bell Syst .Tech.j. 35 (1956) 333-347.

[11] V.Lehann and u. Gosel ,porous silicon formation a quantum wire effect, Appl.Phys.Lett 58 (1991) 856-858.

[12] V. Lehmann, R. Stengl and A. Luigart, On the morphology and the electrochemical formation mechanism of mesoporous silicon ,Mater Sci.Eng.B. 69 (1996) 11-22.

[13] V.Lehmann and S.Ronnebeck, The physics of macropore formation in low doped p- type silicon ,J.Electrochem.soc .146 (1999) 2968-2975.

[14] V. Lehmann and H. Foll., Formation Mechanism and properties of Electrochemically Etched Trenches in n-Type Sillicon , J.Electrochem. Soc. 137 (1999) 653-659.

[15] V. lehmann., The Physics of Macropre Formation in Low Doped n- Type Sillicon, J. Electrochem. 140 (1993) 2836-2843.

[16] D.K. Salucha and A.J. Marchkevicius, Investigation of Porous Layers Passivation Coatings for High Sillicon Devices , Elect ronics rical Eng . 7 (2007) 41-44.

[17] Nichiporuk, O.A. Kaminski, M.Lemiti, A.Fave, S.Litvinenko, V. Skryshevsky, Passivation of the surface of rear contact solar by porous silicon , Thin Solid Films . 512 (2006) 248-251.

[18] Bratkowski, A.A. Korcala , Z. Eukasiak , P. Borowski and W.Bala , Novel GassSensors Based on Porous Sillicon measured by photovoltage , photoluminescence,and admittance Spetroscopy, Opto –Electron Rev. 13 (2005) 35-38.

[19] S. Yaakob , M.A. Bakar, J. Ismail, N.H.H.A. B akar and K.Ibrahim, The formation and morphology of highly doped n-type porous silicon : Effect of short etching time at high current density and avidence of simultaneous chemical and electrochemical dissolutions, J. Phys.Sci. 23 (2012) 17-31.

[20] K. Behzad , W. Yunus, and Z. Talib , Effect of Preparation Parameters on Physical Thermal and Optical Properties of n-type Porous Sillicon , Int.J. Electrochem. Sci. 7 (2012) 8266-8275.

[21] B. L. Sharma and AR. K. Purohit, Semiconductor Heterojunction , Oxford, 1974.

[22] W. C. Wong and H. L. Kwok, Transition from Schottky barriers to p-n junctions, Solid-State Electron. 30 (1987) 719-722.

[23] Raid A. Ismail, Fabrication and Characterization of Photodetector Based on Porous Sillicon , Surf . Sci Nanotech. 8 (2010) 388-391.